Penerbit Akademia Baru

Open Access

A CFD Mesh Independent Solution Technique for Low Reynolds Number Propeller

Aravind Seeni[1], Parvathy Rajendran[1,*], Hussin Mamat[1]

[1] School of Aerospace Engineering, Universiti Sains Malaysia, Engineering Campus, 14300 Nibong Tebal, Pulau Pinang, Malaysia

ARTICLE INFO	ABSTRACT
	There are several techniques available for finding mesh independent solutions in Computational Fluid Dynamics (CFD) problems. The most commonly known methods are the Grid Resolution method, General Richardson Extrapolation and Grid Convergence Index methods. In a problem where the solution of a propeller operating at a chord Reynolds number of roughly between 4000 and 17000 (estimated at 75% radial distance), only an unstructured meshing could be performed. Existing methods presented inadequacies in generating a grid independent solution for such a case. Therefore, a new method namely "Fitting method" is introduced to overcome these inadequacies. The new method uses a polynomial fit to thrust and torque solutions of different mesh refinements. A second order polynomial that fits better with less divergence is used and proposed. The maxima value of the polynomial is deemed the mesh independent solution. For our APC10x7SF low Reynolds number propeller performance estimation, the fitting method was able to successfully provide solutions to a range of advance ratios selected for simulation. The simulation is performed for 14 cases of advance ratios ranging from 0.192 to 0.799. The results when compared with experimental results available in literature provide a successful validation of the proposed method due to satisfactory correlation. When compared with experimental results, less than 10% error was observed for 6 cases of advance ratios, in the case of thrust coefficient whereas there is over-prediction or under-prediction of results for the remaining advance ratios. In the case of torque coefficient, less than 10% error was found for three cases of advance ratios while there is over-prediction for remaining advance ratios. The results through implementation of this method will improve with increasing number of mesh refinements. The method apart from successfully providing a mesh independent solution avoids the difficulty of costs associated with running tests using very fine meshes.

1. Introduction

The reliability of computational prediction of results is a growing concern in CFD scientific community. Some of the major questions thus arise are: Are computational results reliable? How can one assess the accuracy or validity of CFD predictions? What confidence level could be assigned to

---

Corresponding author.
E-mail address: aeparvathy@usm.my (Parvathy Rajendran)

computer predictions? These questions are asked due to the uncertainty associated with the results generated by CFD. Hence verification and validation procedures have been developed to address this growing problem. Verification involves both code verification and solution verification. Verification can be done through analytical, highly accurate hybrid analytical-numerical and manufactured solutions of the mathematical models. Validation typically involves determination of the accuracy of the mathematical model in representing physical phenomena of interest using experimental data that are specially designed and undertaken for this purpose [1]. The principal requirement of the verification and validation procedure is the grid independent numerical solutions, typically performed through extrapolation procedures.

There are three commonly known methods available for determining grid independent solutions. They are 1) Grid resolution method, 2) General Richardson Extrapolation Method and 3) Grid Convergence Index. In Grid Resolution method, the mesh size is determined based on prior knowledge of the physics of the problem. The mesh size is increased incrementally until there is no further significant performance increase with improvement in mesh size [2]. In other words, the optimum grid size above which with further increment in grid size not affecting the quality of results drastically is determined [3].

The second method namely, Generalized Richardson Extrapolation method (GRE) uses an expansion series to determine the exact values. It relies on convergence and refinement rate to estimate the exact solution from the expansion series of errors. An expansion series that consists of the performance estimation variable, grid refinement ratio and order of accuracy will be used. The order of accuracy is calculated by the ratio between logarithmic forms of thrust coefficient differences and grid refinement ratio for uniform grid refinements [4]. For non-uniform grid refinements, the estimation is through solving a transcendental equation [5].Condition to satisfy for using this method is monotonic convergence. Another condition that must be met is that solutions should be asymptotic.

The third method is the Grid Convergence Index (GCI) method which was proposed by Roache [5, 6]. It is based on the Richardson Extrapolation method which also requires 3 meshes to estimate the extrapolated values. The method also includes order of accuracy estimation to find extrapolated values [7]. The method also quantifies relative error between mesh refinements as well as extrapolation relative error. A ratio known as the GCI is also estimated by factoring in a Safety Factor [4, 8]. To use this method, it has been found that the desired grid refinement factor should be greater than 1.3. Furthermore, the grid refinement should be done systematically and structured [7].

Currently available grid independence study techniques require a systematic refinement of mesh by doubling the number of cells from one grid to the other. However, in many problems, such as the current problem, a systematic refinement of the grids could be impossible due to geometric complexity. In this paper, a new method to perform grid independency study is proposed. This method can be applied to problems where current methods are found to be infeasible.

2. Review of Grid Independency Studies on Propellers

A review of grid independency techniques implemented in past studies has been performed. Studies targeting both aeronautical and marine propellers were considered. The working principle of propellers adopted in either application is the same. The studies differ only in shape of the geometry considered. Therefore, studies on both applications are discussed.

The study by Yangang *et al.,* [9] has performed a CFD analysis of swirl recovery vanes of Fokker 29 propeller. In this study, the validation is performed for thrust and torque coefficients. The grid independence study was performed using the grid resolution method. Three grids of resolution 1.13

(coarse), 1.51 (medium) and 2.02 (fine) million cells were used. The thrust coefficient difference showed negligible change in the values between medium and fine and therefore, medium grid was chosen.

The study by de Giorgi [10] focused on numerical prediction of the performance of a contra-rotating open rotor system for a VTOL airplane. The mesh independence analysis was performed using grid resolution method. Three different refinement levels namely, coarse with 1.56 million, medium with 2.46 million and fine with 3.92 million cells were adopted. The results showed that medium sized mesh achieved grid independence for thrust and torque.

The study by Kutty *et al.,* [11] was on 3D simulation and validation of APC Slow Flyer Propeller. In this study, five different mesh sizes namely standard, coarse, mid, mid-fine and fine were used to perform a numerical simulation of a propeller operating at 3008 rpm. The mesh independence study was performed using grid resolution method. Five different meshes of varying density namely standard (0.38 million), coarse (1 million), mid (2 million), mid-fine (3 million) and fine (4 million) were used. It was found that the thrust coefficient (K_T), torque coefficient (K_Q) and efficiency (η) did not approach the asymptotic range. Furthermore, standard mesh produced results of reasonable accuracy relatively closer to experimental and therefore was selected as preferred mesh for further calculations.

Yongle *et al.,* [12] has performed a CFD investigation of tip clearance effects on the performance of a ducted propeller. The mesh independence study was performed using grid resolution method. Three different mesh sizes coarse, medium and fine were employed. The thrust coefficient was found to be least differing with improvement in mesh density beyond medium refinement size. The medium refinement grid was selected for thrust and torque coefficient estimations on the basis of computational efficiency and accuracy consideration.

Yao [13] has performed a CFD investigation of a marine propeller in oblique flow by solving RANS equations. The grid independence study was performed using grid resolution method. Three different grid sizes coarse, medium and fine grid, which has roughly 1.5, 2.6 and 5.2 million cells respectively, was employed to study the thrust and torque. The result showed that the coarse grid experienced a 0.85% error compared to medium of 0.51% error over fine grid for J=0.4.

In some instances, coarse mesh provided better grid refinement values than finer mesh. Liefvendahl [14] performed analysis of propeller wake instability of a submarine propeller using Large Eddy Simulation. The validation is performed on performance characteristics and wake velocity field. Two mesh refinements, coarse and fine were used to compare with experimental results. The coarse mesh agreed better to experimental values than fine mesh for thrust coefficient. However due to lower velocity in wake a fine mesh was chosen.

Stajuda *et al.,* [15] performed a CFD simulation of a propeller. The thrust and power performance of the propeller were studied. A mesh independence study was conducted using grid resolution method. Three mesh variants with nodes varying between 5 and 12 million were used. The result showed that the observed parameters varied with less than 1% error between the coarse and finest of meshes. So the mesh with lowest number of nodes was sufficient and chosen over other variants.

Berchiche and Janson [16] studied the effects of grid resolution and grid quality for simulating an open-water propeller. Three different grids – coarse, medium and fine with mesh grid densities 0.5, 1.4 and 3.8 million were used. A grid refinement factor of √2 is followed for the meshes. As per the result, the thrust coefficient was found approaching closer to experimental values as the mesh resolution gets finer. However, this was not observed for the torque coefficient. A Richardson extrapolation and standard GCI method was subsequently employed to determine grid independency. It was found that the order of accuracy, p was non-uniform for all parameters. The variation in p suggested that not all the data was found in asymptotic range.

Lu *et al.,* [17] performed a CFD simulation to study the hydrodynamic performance of a propulsor. For the grid independence study, no specific method was used. Instead, three conditions of advance ratio were selected for inspection of hydrodynamic performance. The result showed that refined grid resulted in higher computational cost and decrease in grid quality. The coarser unrefined grid was subsequently selected over the refined grid option.

Queutey *et al.,* [18] has conducted a RANS simulation study of ship-propeller interaction using sliding grids and adaptive grid refinement method. The study includes a grid convergence study conducted on five meshes of increasing size namely, 0.775, 1.87, 3.86, 6.97 and 11.4 million. The grid independence study was conducted for a specific advance ratio case for thrust and torque coefficients by calculating the error percentage in comparison with experimental results. The results showed that the numerical error was least for the finest grid.

In Yao and Zhang [19], a grid refinement study based on propeller thrust coefficient estimation was performed as part of the numerical study of propeller exciting bearing forces under non-uniform ship's nominal wake. Three sets of mesh were employed. The grid refinement study was performed by studying the relative percentage difference between the finest and less finer grids. This is an inverse version of the grid resolution method where finest grids tend to become more accurate. The relative percent difference was found to be within 3% when the number of cells increases from 3.12 to 4.39 million. It concluded that the numerical results were little affected by the mesh resolution when the cell number is up to 4.12 million, thus attaining mesh independence.

Yao and Zhang [20] has conducted a CFD study for two cases of propellers rotating after a stern and hull. The study's goal was to measure the exciting forces when operated in a ship's wake condition. Grid refinement study was conducted on the thrust coefficient for a propeller after the stern. This study is performed by estimating the percentage difference between the finest and coarse grids. Three different mesh sizes were simulated and studied for advance ratio, J of 0.6 condition. The study showed when the mesh elements increase from 1.51 to 3.58 million, the observed percentage difference is 6.87%. When the mesh elements increase from 3.58 to 8.56 million the percentage reduced to 1.58%. The results suggested that increasing mesh size made little improvement to numerical results.

Kaidi *et al.,* [21] performed a steady state CFD simulation based on RANS equations to simulate the flow around the hull, propeller and rudders of an Inland Container Ship. In order to test mesh independence using the grid resolution method, three different mesh sizes of increasing tetrahedral element size, 0.96, 1.9 and 3.9 million were employed with a refinement ratio of √2. The propeller mesh sensitivity verification was found to be done by estimating the relative percentage different between numerical and experimental results for K_T, K_Q and η. The medium grid was chosen due to satisfactory estimation of errors and applied for further performance studies on varying advance ratios.

Shora *et al.,* [22] conducted a CFD study to predict the performance and cavitation volume of a marine propeller under different geometrical and physical conditions. In this study, grid independency study for different grid sizing is performed for a 4-bladed B-series propeller using grid resolution method. The grid resolution study helped to identify the ideal grid size of 0.00088 corresponding to 10895632 elements in total based on the results of thrust coefficient variation.

Razaghian and Ghassemi [23] performed a numerical analysis of the hydrodynamic performance of a ducted propeller. The thrust performance was analysed using the grid resolution method. The mesh cell numbers were varied from 4.3 to 9.1 million. It was found that the thrust values stabilize at 9.1 million mesh size.

Majdfar *et al.,* [24] performed a performance prediction on a ducted propeller using RANS. Grid resolution method was utilized to determine the thrust coefficient for one advance ratio. It was found

that the thrust coefficient values do not vary significantly beyond an increase in grid size of 1.4 million.

Zhang *et al.,* [25] performed a CFD study on performance investigation of a ducted propeller in oblique flow. A mesh independence study was conducted to predict numerical uncertainty and also produce results from practical viewpoint for validation. Five mesh grids of increasing mesh element sizes were compared and the relative difference to experimental data was computed. The mesh with highest density was chosen for detailed analysis.

Mizzi *et al.,* [26] demonstrated an approach for optimizing Propeller Box Cap Fins (PBCF) using CFD analysis. First, the CFD model used for PBCF was validated using a model propeller namely Potsdam VP1304. For this purpose, the numerical data was compared with experimental results and the accuracy of convergence estimate based on percentage. The finest mesh was chosen based on the results. Then the Potsdam Propeller Test Case propeller CFD results verification was performed through GCI method. The performance coefficient K_T and K_Q were analysed and verified for uncertainty for three grid sizes namely coarse, medium and fine. A grid refinement ratio of $\sqrt{2}$ was used between medium to coarse grids as well as for fine to medium grids. A monotonic convergence was observed. The results showed insignificant uncertainties of GCI in the thrust and torque coefficient values estimated.

Wang *et al.,*[27] performed a numerical analysis of marine propeller exciting force in oblique flow using CFD. A mesh resolution study was conducted using Grid resolution method for K_T and K_Q by varying the mesh y^+ value between 20 and 100. The result showed that K_T showed greater deviation for mesh with y^+ between 60 and 100. However, the deviation was negligible for mesh with y^+ between 20 and 60. This mesh with $y^+=60$ was chosen as appropriate grid. The total number of elements for this grid size is 3.24 million.

A summary of above discussed studies that have used grid independency techniques for propeller performance analysis is provided in Table 1.

From the literature review, it can be found that most studies use one of the three existing methods to perform grid independence tests. In most studies, the grid resolution method was employed. Some studies have also used GCI method and Standard Richardson Extrapolation method. In some studies, the error percentage between numerical and experimental data is performed. Other studies have used the decreasing error percentage different between coarsest and finest meshes as a mesh independence method. It was found from some studies that for performing mesh convergence tests of propeller performance, a single advance ratio condition was assumed. On the contrary, some studies have chosen the entire range of advance ratio for performing validation with experimental data. It can be found in Table 1 that one of the mesh refinements used is deemed the grid independent solution based on the degree of variation of performance.

Most of the studies considered in this review work are on marine propellers. This implies most research work has targeted design and development of marine propellers. Very few studies on grid independency exist that have used CFD analysis on aircraft and UAV propellers.

Also it can be found that most of the studies have implemented only three mesh refinements in performing their grid independence studies. The reason could be due to the high computational costs involved in performing simulations at high mesh resolution. Some studies have implemented two while others have implemented five and more mesh refinements. Simulation problems that can afford such high computational requirements can use high number of mesh refinements. Hence, employing at least five or more sets generally increases the mesh sensitivity range and helps determine the mesh independence resolution more accurately.

Table 1
Summary of propeller studies that implemented grid independency techniques

No	Study	Grid Independency Technique used	Type of propeller	Selected mesh refinement	No. of mesh refinements
1	Yangang *et al.,* [9]	Grid resolution method	Aircraft	Medium	3
2	de Giorgi [10]	Grid resolution method	Aircraft	Medium	3
3	Kutty *et al.,* [11]	Grid resolution method	UAV	Coarsest	5
4	Yongle *et al.,* [12]	Grid resolution method	Marine	Medium	3
5	Yao [13]	Grid resolution method	Marine	Medium	3
6	Liefvendahl [14]	Grid resolution method	Marine	Coarse	2
7	Stajuda *et al.,* [15]	Grid resolution method	Aircraft	Coarsest	Not available
8	Berchiche and Janson [16]	Richardson extrapolation, GCI	Marine	Not available	3
9	Lu *et al.,* [17]	Comparison of performance between refined and unrefined grids	Marine	Coarse	2
10	Queutey *et al.,* [18]	% error estimation between numerical and experimental data	Marine	Coarse	5
11	Yao and Zhang [19]	% difference between finest and coarser grid results	Marine	Fine	3
12	Yao and Zhang [20]	% difference between finest and coarser grid results	Marine	Medium	3
13	Kaidi *et al.,* [21]	% error estimation between numerical and experimental data	Marine	Medium	3
14	Shora *et al.,* [22]	Grid resolution method	Marine	Finest	9
15	Razaghian and Ghassemi [23]	Grid resolution method	Marine	Finest	9
16	Majdfar *et al.,* [24]	Grid resolution method	Marine	Coarse	6
17	Zhang *et al.,* [25]	% error estimation between numerical and experimental data	Marine	Finest	5
18	Mizzi *et al.,* [26]	% error estimation between numerical and experimental data, GCI	Marine	Finest	3
19	Wang *et al.,* [27]	Grid resolution method	Marine	Medium	9

3. Methodology

3.1 Modelling and Simulation

In this section, the selection of propeller model and the selection of technique for performing simulation will be elaborated.

3.1.1 Propeller geometry

The baseline propeller considered is the Applied Precision Composites (APC) 10x7 Slow Flyer (SF). This propeller is considered due to prior availability of experimental data in literature [28]. It is a two-bladed propeller with a diameter of 0.254 m. The propeller is modelled using CAD software. The geometric modelling of the propeller in chordwise and spanwise directions is performed with specifications available in

Table **2**. The blade consists of two airfoil sections. Sections closer to the hub are designed with Eppler E63 airfoil and sections away from the hub and closer to the tip are designed with Clark-Y. The designed propeller is illustrated in Figure 1.

Table 2
APC10x7SF propeller geometry specifications (r=radial distance, R=propeller radius,c=chord, β=pitch angle)

r/R	c/R	β (°)
0.15	0.109	34.86
0.2	0.132	37.6
0.25	0.155	36.15
0.3	0.175	33.87
0.35	0.192	31.25
0.4	0.206	28.48
0.45	0.216	25.6
0.5	0.222	22.79
0.55	0.225	20.49
0.6	0.224	18.7
0.65	0.219	17.14
0.7	0.21	15.64
0.75	0.197	14.38
0.8	0.18	13.11
0.85	0.159	11.83
0.9	0.133	10.65
0.95	0.092	9.53
1	0.049	8.43

Fig. 1. CAD model of APC10x7SF propeller

3.1.2 Computational fluid dynamics

The flow around the propeller is modelled by steady Reynolds Averaged Navier Stokes Equations (RANS) equations for an incompressible flow. The modelling is performed based on the following principle. The inclusion of a turbulence models generally makes the flow unsteady. RANS turbulence models provide closure to Reynolds Stress tensor that represents the effect of turbulent fluctuations in the mean flow. This allows steady state simulations of turbulent flow being performed in ANSYS Fluent [29].

The CAD model of the propeller will beimported to finite volume based solver namely ANSYS Fluent. Fluent is a CFD software that has been used in several research works in the past [21, 22, 27, 30, 31]. A three-dimensional (3D) computational grid is implemented in which the velocity components u, v and w and pressure component, p at the center of the control volumes is solved. The governing equations consist of the continuity and Reynolds-averaged momentum equation which can be written as follows [21]:

$$\frac{\partial \rho}{\partial t} + \frac{\partial}{\partial x_j}(\rho u_i) = 0 \tag{1}$$

$$\frac{\partial (\rho \overline{u_i})}{\partial t} + \frac{\partial (\rho \overline{u_i u_j})}{\partial x_j} = -\frac{\partial \bar{p}}{\partial x_i} + \frac{\partial}{\partial x_j}\left[\mu\left(\frac{\partial \overline{u_i}}{\partial x_j} + \frac{\partial \overline{u_j}}{\partial x_i} - \frac{2}{3}\delta_{ij}\frac{\partial \overline{u_m}}{\partial x_m}\right)\right] + \frac{\partial}{\partial x_j}\left(-\rho \overline{u_i' u_j'}\right) \tag{2}$$

where δ_{ij} is the Kronecker delta and $-\rho\overline{u_i'u_j'}$ is the Reynolds stresses. The Reynolds stresses could be linked to mean rates of deformation as proposed by Boussinesq hypothesis and can be written as follows [21, 32]

$$-\rho\overline{u_i'u_j'} = \mu_t\left(\frac{\partial u_i}{\partial x_j} + \frac{\partial u_j}{\partial x_i}\right) - \frac{2}{3}\left(\rho k + \mu_t \frac{\partial u_i}{\partial x_i}\right)\delta_{ij} \qquad (3)$$

where μ_t is the turbulent viscosity, μ_t will be estimated by turbulence model equations.

The one-equation Spalart-Allmaras (S-A) is considered as the preferred turbulence model. This is due to the reason that S-A is specifically designed for aerodynamics flows [33] at low Reynolds number [34]. Studies that have implemented S-A in the studies, for example are that of Zhang *et al.,* [25]. The transport model is given by the following equation [35, 36]

$$\frac{\partial \hat{v}}{\partial x} + u_j \frac{\partial \hat{v}}{\partial x_j} = c_{b1}(1 - f_{t2})\hat{S}\hat{v} - \left[c_{w1}f_w - \frac{c_{b1}}{\kappa^2}f_{t2}\right]\left(\frac{\hat{v}}{d}\right)^2 + \frac{1}{\sigma}\left[\frac{\partial}{\partial x_j}\left((v + \hat{v})\frac{\partial \hat{v}}{\partial x_j}\right) + c_{b2}\frac{\partial \hat{v}}{\partial x_i}\frac{\partial \hat{v}}{\partial x_i}\right] \qquad (4)$$

The turbulent eddy viscosity is calculated as follows

$$\mu_t = \rho\hat{v}f_{v1}, \qquad (5)$$

where ρ is the fluid density, $v=\mu/\rho$ is the kinematic viscosity and μ is the dynamic viscosity, and f_{v1} is the viscous damping function which can be expressed as

$$f_{v1} = \frac{X^3}{X^3 + c_{v1}^3} \qquad (6)$$

$$X = \frac{\hat{v}}{v} \qquad (7)$$

The 3D computational domain consists of a rotating frame which is the cylinder enclosing the propeller blade along with the hub. The second frame, the global stationary domain is specified by the enclosure of the smaller cylindrical enclosure. The domain specifications are illustrated in Figure 2(top) and Figure 2(bottom). The domain is modelled in such a way that the intricate flow physics needs are well captured and would not affect the upstream and downstream flow of the propeller.

A distance of 4D between both upstream and downstream ensures the same. Furthermore, a full 3D simulation is ensured with reasonable accuracy without any problems in convergence. The stationary and rotational domains are assigned as translational or rotational zones in ANSYS Fluent. A Multiple Reference Frame approach is followed in which the rotational zone is a moving zone with motion about rotational axis at 3008 rpm. The stationary and rotating domain are separately meshed. Unstructured meshing was performed due to the following reasons. The study by Alakashi *et al.,* [37] showed that both structured and unstructured mesh do not produce significant variation of results in the analysis of a bump channel, NACA0012 airfoil and wind turbine blade using two different codes. The results were found to be similar for both meshes. Furthermore, the study by Shora *et al.,* [22] showed that unstructured mesh was preferred to resolve the boundary layer viscosity effects in the study on novel blade shapes for wind turbine The stationary domain is made of coarse mesh and the blade with finer mesh. This is to ensure that geometries of blade are meshed with better refinement.
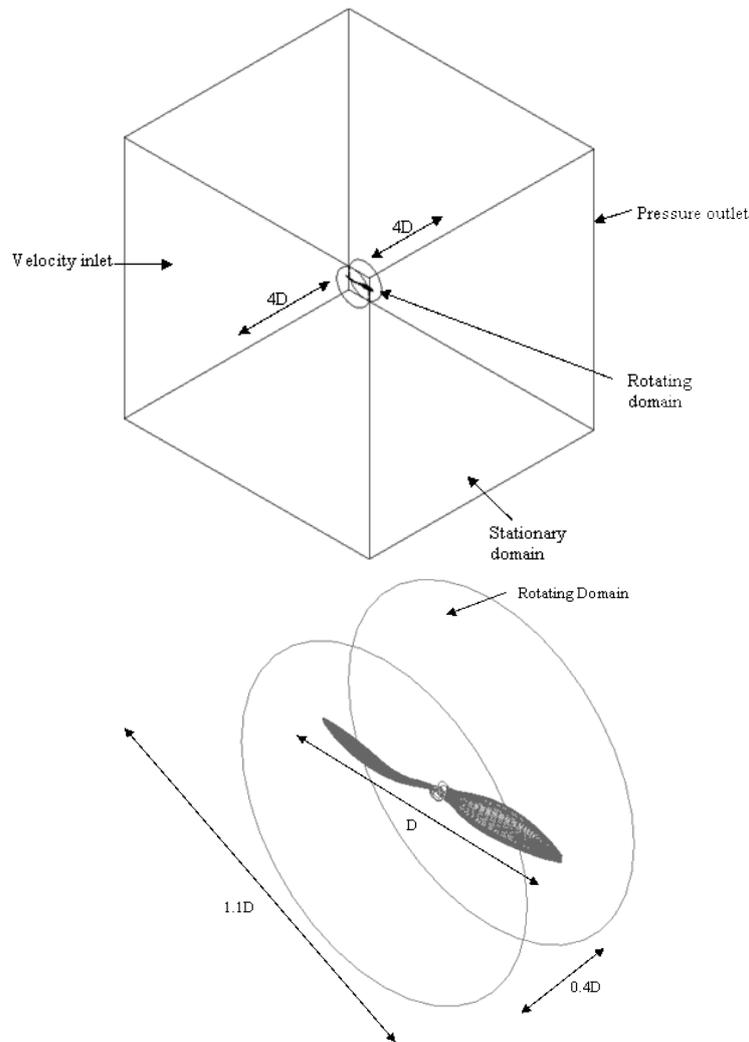
Fig. 2. Computational domain (top); rotational domain with propeller and cylindrical enclosure (bottom)

The mesh consists of unstructured tetrahedron elements. The meshing methodology adopted ensured capturing the complexities associated with the geometry within reasonable amount of time. It was found from earlier section that employing five sets of mesh size generally increases the mesh sensitivity range and helps determine the mesh independence resolution more accurately. The geometry is therefore randomly treated for mesh size improvements from grid M1 to grid M5 for 5 meshes. The sizing of mesh adopted is provided in Table 3.

An airflow velocity is assigned at the inlet with varying speeds. These velocities are assumed based on the experiments by Brandt *et al.,* [28]. The advance ratios and corresponding free stream velocities are listed in Table 4. The advance ratio (J) can be calculated from the following equation

Table 3
Mesh parameters for five grids considered

Grid	Refinement	Total nodes	Total elements	h^2
M1	Standard	41927	199380	0.000154
M2	Coarse	165545	789650	3.88E-05
M3	Medium	242877	1141968	2.68E-05
M4	Mid-fine	292342	1374053	2.23E-05
M5	Fine	798178	3763486	8.14E-06

$$J = \frac{V}{nD} \tag{8}$$

where V is the free stream velocity, n is the rotational speed and D is the diameter. A no slip condition is assumed at the walls. The pressure outlet is allocated with a gauge pressure of 0.

The thrust coefficient can be expressed as follows

$$K_T = \frac{T}{\rho n^2 D^4} \tag{9}$$

where T is the thrust, ρ is the density. The torque coefficient can be expressed as follows

$$K_Q = \frac{Q}{\rho n^2 D^5} \tag{10}$$

where Q is the torque

Table 4
Advance ratios and corresponding free stream velocities

Case	Advance ratio, J	Free stream velocity, V (m/s)
1	0.192	2.4384
2	0.236	2.9972
3	0.282	3.5814
4	0.334	4.2418
5	0.383	4.8641
6	0.432	5.4864
7	0.486	6.1722
8	0.527	6.6929
9	0.573	7.2771
10	0.628	7.9756
11	0.659	8.3693
12	0.717	9.1059
13	0.773	9.8171
14	0.799	10.1473

The simulation settings are set as follows; a "coupled" scheme with a Semi-Implicit Method for Pressure-Linked Equations (SIMPLE) is set for pressure-velocity coupling. A Least-Squares Cell-based algorithm is assigned for gradients. The pressure is assigned with Standard scheme of interpolation. A second order upwind interpolation scheme is used for momentum, Turbulent Kinetic Energy and Turbulent Dissipation Rate. Convergence of simulation iteration was determined by the order of magnitude of the residuals. The drop of all scaled residuals below 1×10^{-4} was utilized as the convergence criterion. The maximum number of iterations in a time step was set as 500 which was found to be sufficient for the residuals to attain convergence.

3.2 Fitting Method

The grid resolution method could not be used due to the results not approaching values of fine mesh refinement i.e. the values not achieving asymptotic range (see Figure **3**). The standard Richardson extrapolation method requires that the mesh is uniformly refined and refined by a factor of two [4]. Also it was found that in the Richardson extrapolation method the grid convergent values

do not try to achieve desired asymptotic range. Therefore, this method does not serve the purpose as the meshes are non-uniformly refined.
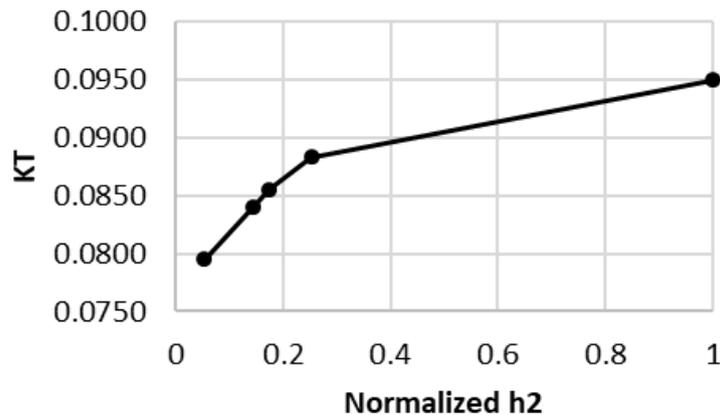

Fig. 3. Inadequate grid independent solution of thrust coefficient (K_T) for J=0.383 through grid resolution method

The GCI method requires that the desired grid refinement factor should be greater than 1.3. The grid refinement should also be done systematically and be structured [7]. Due to these reasons, the GCI method cannot be used for the given problem. Existing methods are found to be inadequate for the problem with data from non-uniform mesh sizes.

Another method will be therefore proposed known as the fitting method. The fitting method was originally proposed in Almohammadi *et al.,* [2]. As per the proposed method, the mesh independent solution of power coefficient of a wind turbine can be determined from curve fitting of data. Data generated from mesh sizes are first plotted versus representative cell size of corresponding mesh sizes. The square of the representative mesh size (h^2) can be expressed as follows:

$$h^2 = \frac{V}{N} \tag{11}$$

where h^2 is the ratio between mesh volume (V) and number of elements (N) for each mesh refinement. The intersection of power coefficient curve at y where h^2=0 was deemed to be the mesh independent solution of power coefficient.

The study also presented two schemes, first order and second order in which both first order and second order polynomials fit to power coefficient data. However, the method proposed by Almohammadi *et al.,* [2] had a drawback. It did not provide a detailed explanation into the reason behind choosing mesh independent results at h^2=0. Also, this method may not be suitable for data with non-uniform mesh sizes. In this work, these drawbacks have been addressed using a modified technique.

Here, in the current method, the performance variation versus mesh size data is fitted to a curve of suitable polynomial order. The first and second order polynomial for thrust coefficient, K_T estimation can be written as a function of the mesh size as follows in respective order:

$$K_T = Ah^2 + B \tag{12}$$

$$K_T = A(h^2)^2 + Bh^2 + C \tag{13}$$

where A, B and C are the coefficients and h^2 is the square of the representative cell size. The maxima existing in the curve can be declared the mesh independent solution due to the reason that the curve follows a polynomial with maxima in case of thrust coefficient. The same could be applied if a minima condition exists. The corresponding mesh size and number of cells required can be estimated. The mesh independent number of elements required to perform the analysis can be determined from Eq. 13.

4. Results and discussion

The performance values measured are the thrust and torque of the propeller. The simulation runs were performed for five different mesh sizes namely standard, coarse, medium, mid fine and fine with mesh sizes from high to low. Prior studies have used experimental data as reference data [28] which were then used to compare with numerical data. This procedure does not provide a mesh independent solution.

The process of performing mesh independency study is to find solutions with no exact solution available a priori. It is performed to validate the numerical solution by employing appropriate techniques and find the optimal mesh size and solution. Experimental data can only be compared after estimation of these mesh independent solutions.

The fitting method was employed in this work in determining mesh independent solution of thrust and torque performance of a propeller. It was performed by curve fitting data to first order and second order polynomials. All advance ratio conditions were considered. The curve fit of K_T is provided in Figure 4 and K_Q in Figure 5. The K_T can be plotted for different mesh sizes and can be made available in a graphical form. The data can be supposed to remain in a linear relation polynomial of first order.

If the data are scattered and do not fit in a linear relationship, then the second order polynomial could be used. The mesh independent K_T is now the maxima of the polynomial function. This is true since the K_T varies with mesh size non-linearly but in suitable order. The point where the curve ascends and descends is the point of mesh independency. This is simply the point where the slope of the curve is zero. The K_T from the mesh independent solution is the maxima if the curve ascends and descends or minima, if vice versa.
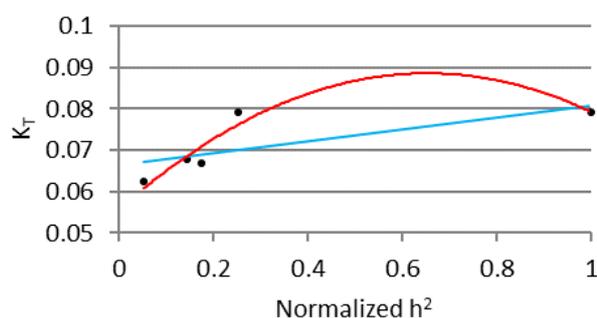

Fig. 4. APC10x7SF propeller's thrust coefficient data fitting to first order (in "blue") and second order (in "red") polynomial for *J*=0.486
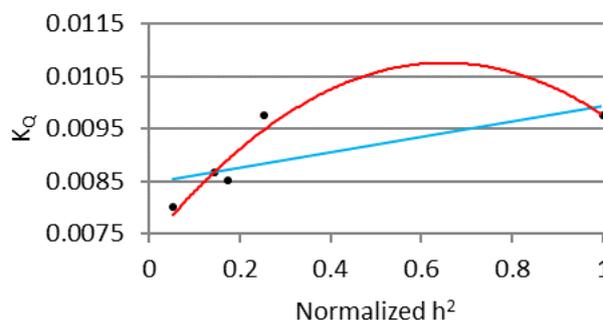

Fig. 5. APC10x7SF propeller's torque coefficient data fitting to first order (in "blue") and second order (in "red") polynomial for J=0.486

It can be found that the first order curve fit was found to be highly divergent with R^2=0.52 for K_T and R^2=0.51 for K_Q. A second order polynomial curve was able to provide a reasonable data convergence (R^2=0.88 for K_T and R^2=0.89 for K_Q). So a second order fit was preferred. The *y* values in all curves have an increasing and then decreasing curve. This was observed for all advance ratios.

There is a point in which increasing and decreasing transition takes place. The maxima of the fitting function are the mesh independent solution. The corresponding value of *x* provides the independent mesh size required. The thrust performance can now be plotted as a mesh independent solution in Figure 6. The corresponding mesh size was found to be 0.00999. Similarly, the torque performance can be plotted as in Figure 7.
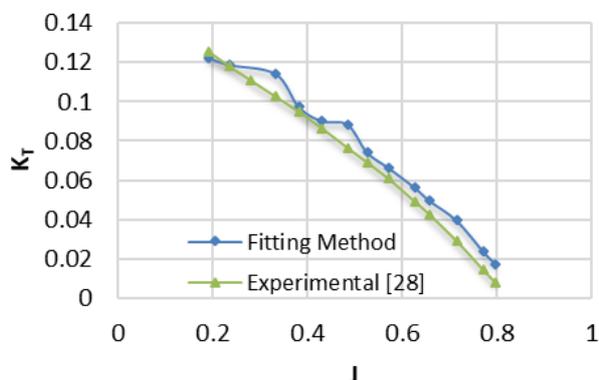

Fig. 6. Grid independence solution of thrust coefficient using Fitting Method in comparison to experimental data
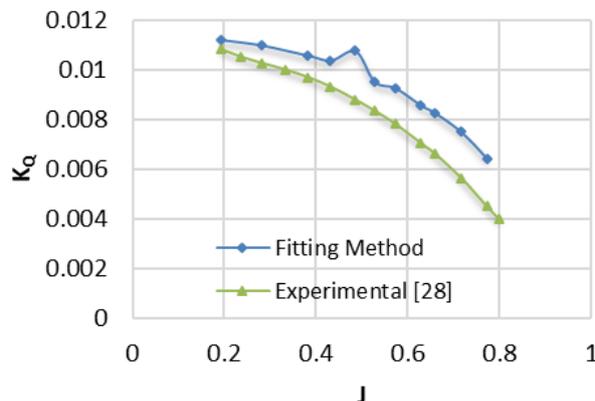
Fig. 7. Grid independence solution of torque coefficient using Fitting Method in comparison to experimental data

It was found from Figure 6 and Figure 7 that there is over-prediction of mesh-independent K_Q results for Case 7 condition of J=0.486. The same could be observed for Case 4 and Case 7 in the estimation of K_T. This error could be due to the non-availability of sufficient number of grid refinements. An inclusion of additional number of grid refinements could solve the problem of over- as well as underprediction of results.

The relative error percentage of K_T and K_Q between the fitting method and experimental results can be calculated through the expressions provided in Eq. 14 and 15

$$\Delta K_T(\%) = \left| \frac{K_{T_{CFD}} - K_{T_{EXP}}}{K_{T_{EXP}}} \right| \times 100 \tag{14}$$

$$\Delta K_Q(\%) = \left| \frac{K_{Q_{CFD}} - K_{Q_{EXP}}}{K_{Q_{EXP}}} \right| \times 100 \tag{15}$$

The error between the fitting method generated results and experiments are summarized in Table 5. It can be found from graph in Figure 6 that the results generated using the new method follow the experimental results' data trend closely with a relative error percentage of below 10% for 6 cases of advance ratiosfor $K_T$whereas there is over-prediction or under-prediction of results for the remaining advance ratios. In the case of K_Q, less than 10% error was found for three advance ratios while there is over-prediction for remaining advance ratios. While the use of other three methods proposed in previos studies [6 – 8] are acceptable only for structured grids with uniform mesh refinements, they provide higher error estimates than the current method. Nonetheless, Figure 7 produced a higher error percentage for $K_Q$and it seems that the error percentage increased with increasing advance ratios. The high error percentage is due to the reason that K_Q is a miniscule quantity. Also the increase in error with advance ratio between numerical and experimental results could be due to the reason that the Reynolds number is increasing as freestream velocity increased. Note that this method is

proposed for low Reynolds number. Nevertheless, the fitting method follow a similar data trend as experiment. Consequently the accuracy of CFD prediction is enhanced using the proposed method.

Table 5
Error percentage of CFD and experimental methods

J	Error %	
	ΔK_T (%)	ΔK_Q (%)
0.192	2.60	3.6
0.236	0.67	48.9
0.282	15.95	7.0
0.334	11.32	73.9
0.383	2.51	9.1
0.432	4.39	11.4
0.486	15.62	22.3
0.527	7.54	13.9
0.573	9.41	18.5
0.628	14.39	21.5
0.659	16.92	24.7
0.717	36.40	32.7
0.773	67.09	42.7

The accuracy of this method increases with implementation of more number of grid refinements. The above presented method of curve fitting provides useful applications to available existing methods: One reason is that the computational expense to find the optimal mesh size and solution is prohibitive in problems employing huge number of cells. This method saves the computational costs of using much finer meshes. Secondly, this method allows finding the solution for unstructured grid refinements.

5. Conclusion

An alternate method known as the fitting method was proposed in order to provide reliable estimations of grid independent solutions in CFD analysis. The method was able to predict the thrust and torque performance accurately for an APC10x7SF low Reynolds number propeller. In this method, polynomial fits of suitable order are used to fit data for different mesh refinements. The given polynomial functions were deemed the mesh refinement solution. This method was able to reliable identify mesh independent solutions for the thrust and torque performance of a propeller operating at 3008 rpm. A reliable verification method was therefore found for this propeller performance estimation in this study.

References
[1] Baliga, Bantwal R., and Iurii Yuri Lokhmanets. "Generalized Richardson extrapolation procedures for estimating grid-independent numerical solutions." *International Journal of Numerical Methods for Heat & Fluid Flow* 26, no. 3/4 (2016): 1121-1144.
[2] Almohammadi, K. M., D. B. Ingham, L. Ma, and M. Pourkashan. "Computational fluid dynamics (CFD) mesh independency techniques for a straight blade vertical axis wind turbine." *Energy* 58 (2013): 483-493.

[3]   Kumar, P. Madhan, Paresh Halder, Abdus Samad, and Shin Hyung Rhee. "Wave Energy Harvesting Turbine: Effect of Hub-To-Tip Profile Modification." *International Journal of Fluid Machinery and Systems* 11, no. 1 (2018): 55-62.

[4]   Roy, Christopher J. "Review of code and solution verification procedures for computational simulation." *Journal of Computational Physics* 205, no. 1 (2005): 131-156.

[5]   Roache, Patrick J. "Quantification of uncertainty in computational fluid dynamics." *Annual review of fluid Mechanics* 29, no. 1 (1997): 123-160.

[6]   Roache, Patrick J. "Perspective: a method for uniform reporting of grid refinement studies." *Journal of fluids engineering* 116, no. 3 (1994): 405-413.

[7]   Celik, Ishmail B., Urmila Ghia, Patrick J. Roache, and Christopher J. Freitas. "Procedure for estimation and reporting of uncertainty due to discretization in CFD applications." *Journal of fluids Engineering-Transactions of the ASME* 130, no. 7 (2008).

[8]   Roache, Patrick J. *Verification and Validation in Computational Science and Engineering.* New York: Hermosa Publishers, New Mexico, 1998.

[9]   Wang, Yangang, Qingxi Li, G. Eitelberg, L. L. M. Veldhuis, and M. Kotsonis. "Design and numerical investigation of swirl recovery vanes for the Fokker 29 propeller." *Chinese Journal of Aeronautics* 27, no. 5 (2014): 1128-1136.

[10]   De Giorgi, Maria Grazia, Teresa Donateo, Antonio Ficarella, Donato Fontanarosa, Anna Eva Morabito, and Luca Scalinci. "Numerical investigation of the performance of Contra-Rotating Propellers for a Remotely Piloted Aerial Vehicle." *Energy Procedia* 126 (2017): 1011-1018.

[11]   Kutty, Hairuniza, and Parvathy Rajendran. "3d cfd simulation and experimental validation of small apc slow flyer propeller blade." *Aerospace* 4, no. 1 (2017): 10.

[12]   Yongle, Ding, Song Baowei, and Wang Peng. "Numerical investigation of tip clearance effects on the performance of ducted propeller." *International journal of naval architecture and ocean engineering* 7, no. 5 (2015): 795-804.

[13]   Yao, Jianxi. "Investigation on hydrodynamic performance of a marine propeller in oblique flow by RANS computations." *International Journal of Naval Architecture and Ocean Engineering* 7, no. 1 (2015): 56-69.

[14]   Liefvendahl, Mattias. "Investigation of propeller wake instability using LES." *Ship Technology Research* 57, no. 2 (2010): 100-106.

[15]   Stajuda, Mateusz, Maciej Karczewski, Damian Obidowski, and Krzysztof Jóźwik. "Development of a CFD model for propeller simulation." *Mechanics and Mechanical Engineering* 20, no. 4 (2016): 579–593.

[16]   Berchiche, Nabila, and Carl-Erik Janson. "Grid influence on the propeller open-water performance and flow field." *Ship Technology Research* 55, no. 2 (2008): 87-96.

[17]   Lu, Lin, Guang Pan, and Prasanta K. Sahoo. "CFD prediction and simulation of a pumpjet propulsor." *International Journal of Naval Architecture and Ocean Engineering* 8, no. 1 (2016): 110-116.

[18]   Queutey, Patrick, Garbo Deng, Jeroen Wackers, Emmanuel Guilmineau, Alban Leroyer, and Michel Visonneau. "Sliding grids and adaptive grid refinement for RANS simulation of ship-propeller interaction." *Ship technology research* 59, no. 2 (2012): 44-57.

[19]   Yao, Huilan, and Huaixin Zhang. "Numerical Studies of Propeller Exciting Bearing Forces under Nonuniform Ship's Nominal Wake and the Influence of Cross Flows." *Shock and Vibration* 2017 (2017).

[20]   Yao, Huilan, and Huaixin Zhang. "Numerical simulation of two experiments for studying propeller exciting forces." *Ships and Offshore Structures* 13, no. 5 (2018): 532-539.

[21]   Kaidi, S., H. Smaoui, and P. Sergent. "CFD Investigation of Mutual Interaction between Hull, Propellers, and Rudders for an Inland Container Ship in Deep, Very Deep, Shallow, and Very Shallow Waters." *Journal of Waterway, Port, Coastal, and Ocean Engineering* 144, no. 6 (2018): 04018017.

[22]   Shora, Mohammad Mahdi, Hassan Ghassemi, and Hashem Nowruzi. "Using computational fluid dynamic and artificial neural networks to predict the performance and cavitation volume of a propeller under different geometrical and physical characteristics." *Journal of Marine Engineering & Technology* 17, no. 2 (2018): 59-84.

[23]   Razaghian, Amir Hossein, and Hassan Ghassemi. "Numerical analysis of the hydrodynamic characteristics of the accelerating and decelerating ducted propeller." *Zeszyty Naukowe Akademii Morskiej w Szczecinie* 47 (119) (2016): 42-53.

[24]   Majdfar, Sohrab, Hassan Ghassemi, Hamid Forouzan, and Arash Ashrafi. "Hydrodynamic prediction of the ducted propeller by CFD solver." *Journal of Marine Science and Technology* 25, no. 3 (2017): 268-275.

[25]   Zhang, Qin, Rajeev K. Jaiman, Peifeng Ma, and Jing Liu. "Investigation on the performance of a ducted propeller in oblique flow." *Journal of Offshore Mechanics and Arctic Engineering* 142, no. 1 (2020).

[26]   Mizzi, Kurt, Yigit Kemal Demirel, Charlotte Banks, Osman Turan, Panagiotis Kaklis, and Mehmet Atlar. "Design optimisation of Propeller Boss Cap Fins for enhanced propeller performance." *Applied Ocean Research* 62 (2017): 210-222.

[27]   Wang, Chao, Shengxia Sun, Shuai Sun, and Liang Li. "Numerical analysis of propeller exciting force in oblique flow." *Journal of Marine Science and Technology* 22, no. 4 (2017): 602-619.

[28]   Brandt, J. B., and M. S. Selig. "Small-scale propeller performance at low speeds–Online Database." (2010).

[29]   Davoudabadi, Peyman. "The Most Accurate and Advanced Turbulence Capabilities." In *Confidence by Design Workshop Chicago, IL, June*, vol. 14. 2012.

[30]   Paik, Kwang-Jun, Seunghyun Hwang, Jaekwon Jung, Taegu Lee, Yeong-Yeon Lee, Haeseong Ahn, and Suak-Ho Van. "Investigation on the wake evolution of contra-rotating propeller using RANS computation and SPIV measurement." *International Journal of Naval Architecture and Ocean Engineering* 7, no. 3 (2015): 595-609.

[31]   Villalpando, Fernando, Marcelo Reggio, and Adrian Ilinca. "Assessment of turbulence models for flow simulation around a wind turbine airfoil." *Modelling and simulation in Engineering* 2011 (2011): 6.

[32]   ANSYS. "Lecture 7: Turbulence Modeling, Introduction to ANSYS Fluent." ANSYS, Inc., (2014): 46.

[33]   Spalart, Philippe, and Steven Allmaras. "A one equation turbulence model for aerodynamic flows." *La Rech. Aerosp.* 1 (1994): 5–21.

[34]   Davidson, Lars, Davor Cokljat, Jochen Fröhlich, Michael A. Leschziner, Chris Mellen, and Wolfgang Rodi, eds. *LESFOIL: Large Eddy Simulation of Flow Around a High Lift Airfoil: Results of the Project LESFOIL Supported by the European Union 1998–2001*. Vol. 83. Springer Science & Business Media, 2012.

[35]   C. L. Rumsey. *The Spalart-Allmaras Turbulence Model* 2018.

[36]   Allmaras, Steven R., and Forrester T. Johnson. "Modifications and clarifications for the implementation of the Spalart-Allmaras turbulence model." In *Seventh international conference on computational fluid dynamics (ICCFD7)*, pp. 1-11. 2012.

[37]   Alakashi, Abobaker Mohammed, and Ir Bambang Basuno. "Comparison between structured and unstructured grid generation on two dimensional flows based on Finite Volume Method (FVM)." *Int. J. Min., Metall. Mech. Eng* 2, no. 2 (2014): 97-103.